LBL-32220
UC-414

Lawrence Berkeley Laboratory
UNIVERSITY OF CALIFORNIA

Accelerator & Fusion
Research Division

Presented at the Fourteenth International Free Electron
Laser Conference, Kobe, Japan, August 23–28, 1992,
and to be published in the Proceedings

The Multi-Cavity Free-Electron Laser

S. Krishnagopal, G. Rangarajan, and A. Sessler

July 1992

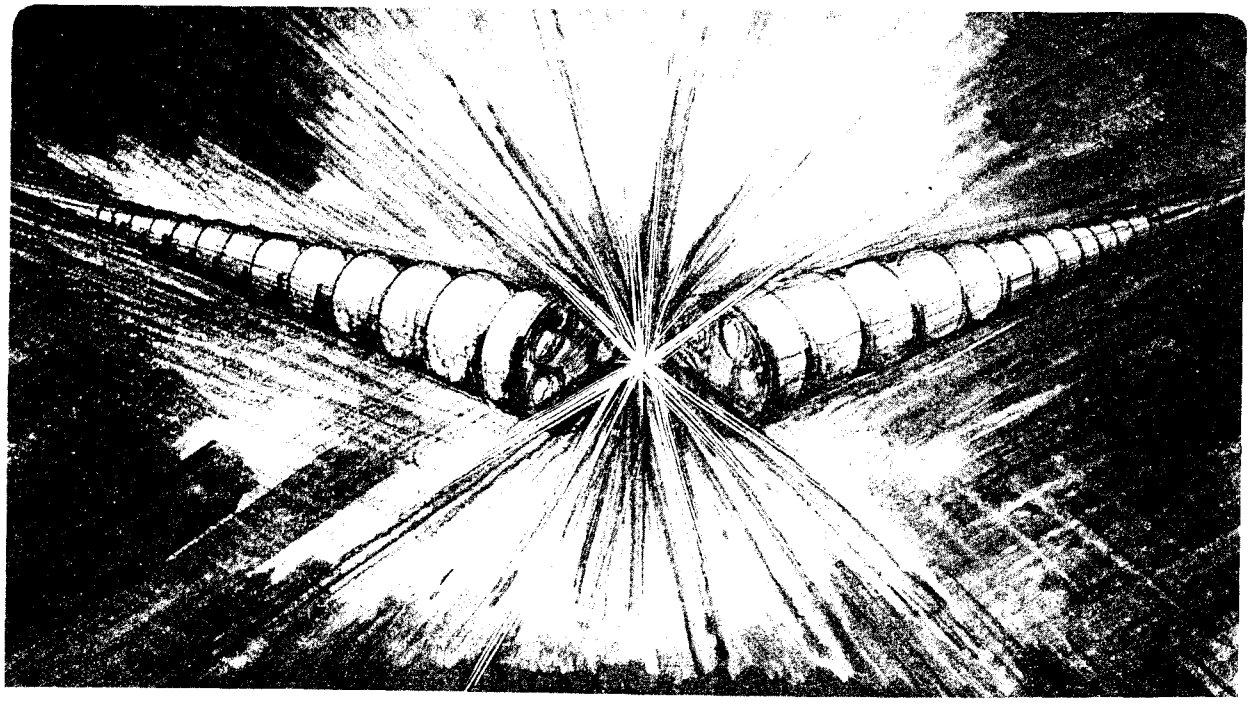

Prepared for the U.S. Department of Energy under Contract Number DE-AC03-76SF00098

LBL-32220
ESG - 180
UC-414

The Multi-Cavity Free-Electron Laser

S. Krishnagopal, G. Rangarajan and A. Sessler*

Lawrence Berkeley Laboratory, University of California, Berkeley, California 94720

July 1992

*Work supported by the Director, Office of Energy Research, Office of High Energy and Nuclear Physics, Division of High Energy Physics, of the U.S. Department of Energy under Contract No. DE-AC03-76SF00098

THE MULTI-CAVITY FREE-ELECTRON LASER*

Srinivas Krishnagopal, Govindan Rangarajan, and Andrew Sessler

Lawrence Berkeley Laboratory
University of California
Berkeley, CA 94720

July , 1992

Consideration is made of a free-electron laser with many optical cavities where the cavities communicate with each other, not optically, but through the electron beam. Analysis is made in the one-dimensional approximation. A general expression is given for the growth rate in the exponential (high current) regime. In the regime where lethargy is important expressions are given in the two opposite limits of small and large numbers of cavities and bunches. Numerical simulation results, still in the one-dimensional approximation, but including non-linearities, are presented. The multi-cavity free-electron laser (MC/FEL) can be employed to avoid the slippage phenomena, and thus to make pico-second pulses of infra-red radiation. Three examples of this application are presented.

* Work supported by the Director, Office of Energy Research, Office of High Energy and Nuclear Physics, Division of High Energy Physics, of the U.S. Department of Energy under Contract No. DE-AC03-76SF00098

1. Introduction

There are many uses for brief, intense pulses of radiation. At long wavelengths it is not possible to directly employ a free-electron laser (FEL) for this purpose since the intrinsic slippage in a FEL, between light and electrons, implies that the light pulse will not be as brief as the electron pulse. One can modify the group velocity (readily done when the wavelength is of the order of the light pipe) and thus make the light pulse stay with the electron pulse, and this has been shown, experimentally, to be possible [1]. This method, group velocity modification, is, however, difficult and, most importantly, limited to rather long wavelengths. Another possibility is to "chirp" the light pulse and then compress it, but this technique is difficult to employ with intense pulses.

Still another possibility is to employ a Multi-Cavity Free-Electron Laser (MC/FEL), and it is this possibility that we want to explore in the present paper. The idea is rather straightforward. One simply makes the FEL optical cavities sufficiently short that the slippage length, in one optical cavity, is less than the electron pulse width. When the electrons reach the end of one cavity they go on to the next, but the radiation remains trapped within that cavity.

In Section 2 we amplify the discussion of the concept; in Section 3 we present the one-dimensional linear analysis; and in Section 4 we describe the numerical simulation and present examples. The final section, Section 5, contains our conclusions.

2. The Concept

The MC/FEL consists of a number of short optical cavities, each with a length less than the slippage distance between the electrons and the radiation. A small hole is drilled at the center of the walls separating the cavities so that the electrons can pass through from one cavity to the next; however, the radiation emitted with a particular cavity remains largely confined within that cavity. Coherent radiation is extracted only from the last cavity. A schematic of the proposed layout is given in Fig. 1.

At first, one might think that the FEL, in a MC/FEL, will not work very well, for its effective length is just an optical cavity length and therefore not very long. However, the electrons, which move on to the next cavity, are bunched and the FEL action in the next cavity is significant.

One is reminded of an optical klystron [2] or of the "gain cavities" in a regular klystron. In fact, in our numerical studies we see that even when the first few cavities have a net loss (so that the gain is not adequate to overcome the mirror losses) the MC/FEL still "works", i.e., the later cavities (which now experience bunched electrons and thus have more gain) are soon experiencing a build-up of radiation to a very high value.

By making the optical cavities confocal, one can reduce the radiation moving from one cavity into the next; i.e., improve the reflection coefficient from the end mirrors (which must have holes for the electron beam to go through). One should note that radiation moving from one cavity to the next is not a serious matter, since the radiation will have slipped out of the electron pulse and therefore no longer be amplified. Just as in a regular klystron, the light is only removed from the last cavity and, thus, the reflection coefficient for this last cavity is much lower than for the other cavities.

3. Linear Analysis

A. Generalities

In this subsection we derive the linearized equations of motion for dynamics in a MC/FEL. We start with the full nonlinear equations of motion which, following the notation of Bonifacio, Pellegrini, and Narducci [3], are

$$\left(\frac{d\theta_j}{dt}\right) = \omega_0\left(1-\gamma_R^2/\gamma_i^2\right)+\frac{1}{2\gamma_i^2\lambda}[JJ]\left[\alpha\exp\left(i\theta_j\right)+c.c.\right] \tag{1a}$$

$$\left(\frac{d\gamma_j}{dt}\right) = \frac{-ec\kappa}{2mc^2\gamma_j}[JJ]\left[\alpha\exp\left(-i\theta_j\right)+c.c.\right] \tag{1b}$$

$$\frac{1}{c}\frac{d\alpha}{dt} = 2\pi n_0\frac{\kappa}{\Sigma}\left\langle\frac{e^{-i\theta_j}}{\gamma_j}\right\rangle. \tag{1c}$$

Here α is the complex amplitude of the electric field, θ_j is the phase of the j^{th} electron relative to the electromagnetic field, and γ_j is its energy in units of mc^2. ω_0 is the wiggler frequency, κ is the wiggler parameter, and λ is the wavelength of the radiation field. The resonant

energy is γ_R, the electron density is n_0 and Σ is the effective transverse cross-section of the beam, describing the overlap of the beam with the radiation field. The average $\langle \ldots \rangle$ is carried over all electrons in the bunch. $[JJ]$ is the usual Bessel function factor that is unity for helical wigglers.

To proceed to a linear analysis, we drop the second term in Eq. (1a) and introduce the variables

$$\Omega_p = \left(4\pi r_e n_0 c^2\right)^{1/2} \tag{2}$$

$$\rho = \frac{1}{\gamma_0}\left[\frac{1}{4\omega_0}\kappa\left(\gamma_0 / \gamma_R\right)^2 \Omega_p\right]^{2/3}, \tag{3}$$

where Ω_p is the plasma frequency and ρ is the FEL parameter. We also rescale the dynamical variables as follows:

$$\tau \equiv 2\omega_0\left(\gamma_R / \gamma_0\right)^2 t \tag{4a}$$

$$\psi_j \equiv \theta_j - \dot{\theta}_0 t \tag{4b}$$

$$\Gamma_j \equiv \gamma_j / (\rho\gamma_0) \tag{4c}$$

$$A \equiv \alpha \exp\left(i\dot{\theta}_0 t\right) / \left(4\pi mc^2 \gamma_0 n_0 \rho^2\right)^{1/2}, \tag{4d}$$

where γ_0 is the input energy.

After recasting the nonlinear equations of motion in these scaled variables, we linearize them around the equilibrium state $A_0 = 0$, $\Gamma_j = 1/\rho$, $\langle \exp(-in\psi_0) \rangle = 0$. We perturb around this equilibrium state by letting $A = a$, $\Gamma_j = (1/\rho)(1 + \eta_j)$ and $\psi_j = \psi_{0j} + \delta\psi_j$, where $\delta = \Delta/\rho$, and Δ is the usual detuning parameter. Then, the linearized equations of motion are [Ref. 3, Eqs. 19-21],

$$\frac{dx}{d\tau} = y \tag{5}$$

$$\frac{dy}{d\tau} = -a \tag{6}$$

$$\frac{da}{d\tau} = -i\delta a - ix - \rho y\,, \tag{7}$$

where the variables x and y are given by

$$x = \left\langle \delta\psi_j \exp(-i\psi_0) \right\rangle, \tag{8a}$$

$$y = \frac{1}{\rho}\left\langle \eta_j \exp(-i\psi_0) \right\rangle. \tag{8b}$$

We look for solutions with an exponential time-dependence, exp $(i\lambda\tau)$, which leads to the characteristic equation

$$\lambda^3 - \delta\lambda^2 + \rho\lambda + 1 = 0\,. \tag{9}$$

Let the solutions to this equation, i.e. the eigenvalues, be λ_1, λ_2, λ_3. Then the general solutions can be written as

$$x(\tau) = x_1 e^{i\lambda_1\tau} + x_2 e^{i\lambda_2\tau} + x_3 e^{i\lambda_3\tau} \tag{10a}$$

$$y(\tau) = y_1 e^{i\lambda_1\tau} + y_2 e^{i\lambda_2\tau} + y_3 e^{i\lambda_3\tau} \tag{10b}$$

$$a(\tau) = a_1 e^{i\lambda_1\tau} + a_2 e^{i\lambda_2\tau} + a_3 e^{i\lambda_3\tau}\,, \tag{10c}$$

where $x_1, x_2, x_3, y_1, y_2, y_3, a_1, a_2, a_3$ are constants. Using the original differential equations (Eqs. 5-7), six of these can be expressed in terms of the remaining three—say x_1,x_2,x_3. These in turn can be expressed in terms of the initial conditions. At $\tau = 0$, let $x = x_{in}$, $y = y_{in}$ and $a = a_{in}$. Then, from the general solutions, (Eqs. 10), we find that

$$x_{in} = x_1 + x_2 + x_3 \tag{11a}$$

$$y_{in} = i\lambda_1 x_1 + i\lambda_2 x_2 + i\lambda_3 x_3 \tag{11b}$$

$$a_{in} = \lambda_1^2 x_1 + \lambda_2^2 x_2 + \lambda_3^2 x_3\,, \tag{11c}$$

from which we can solve for (x_1,x_2,x_3) in terms of (x_{in}, y_{in}, a_{in}).

B. Exponential Gain Regime

We now assume that the FEL is operating in the exponential regime, which corresponds to one of the eigen-functions dominating over the other two; for concreteness we choose it to be the one associated with λ_1. In this regime the solutions Eqs. (10) reduce to

$$x(\tau) = x_1(x_{in}, y_{in}, a_{in})e^{i\lambda_1\tau} \tag{12a}$$

$$y(\tau) = i\lambda_1 x_1(x_{in}, y_{in}, a_{in})e^{i\lambda_1\tau} \tag{12b}$$

$$a(\tau) = \lambda_1^2 x_1(x_{in}, y_{in}, a_{in})e^{i\lambda_1\tau}, \tag{12c}$$

where the explicit form of x_1 is

$$x_1(x_{in}, y_{in}, a_{in}) = \frac{1}{\lambda_1(\lambda_1+\lambda_2+\lambda_3)+\lambda_2\lambda_3}\left[a_{in} + \lambda_2\lambda_3 x_{in} + i(\lambda_2+\lambda_3)y_{in}\right]. \tag{13}$$

Single bunch: We now apply these results to an analysis of the multicavity FEL. Consider such an FEL consisting of N cavities, each of length $L = cT$. Consider a single bunch of electrons passing through the FEL. At the entrance to the first cavity let the initial conditions be $x_{in} = x_0$, $y_{in} = y_0$, $a_{in} = a_0$. We assume that the growth is exponential within the cavity and the dynamics is governed by Eqs. (12). At the end of the cavity the values of x, y and a are

$$x(\tau = T) \equiv x_1^1 = x_1(x_0, y_0, a_0)e^{i\lambda_1 T} \tag{14}$$

$$y(\tau = T) \equiv y_1^1 = i\lambda_1 x_1(x_0, y_0, a_0)e^{i\lambda_1 T} \tag{15}$$

$$a(\tau = T) \equiv a_1^1 = \lambda_1^2 x_1(x_0, y_0, a_0)e^{i\lambda_1 T}, \tag{16}$$

where in x_1^1, y_1^1, a_1^1 the superscript indexes the cavity number and the subscript the bunch number.

The electrons make their way to the second cavity without experiencing any perturbation, so that for the second cavity $x_{in} = x_1^1$ and $y_{in} = y_1^1$. The radiation, on the other hand, remains trapped within the first cavity, so that $a_{in} = a_0$. Applying Eq. (12) again, one can calculate the values x_1^2, y_1^2 and a_1^2 at the end of the second cavity. Repeating this for N cavities one can show that

$$x_1^N = \frac{1}{D^{N-1}}\left(C_x + i\lambda_1 C_y\right)^{N-1} \cdot \frac{1}{D} \cdot \left[a_0 + C_x x_0 + C_y y_0\right] e^{i\lambda_1 NT}, \tag{17}$$

where

$$D = \lambda_1\left(\lambda_1 - \lambda_2 - \lambda_3\right) + \lambda_2\lambda_3 \tag{18a}$$

$$C_x = \lambda_2\lambda_3 \tag{18b}$$

$$C_y = i\left(\lambda_2 + \lambda_3\right). \tag{18c}$$

It is instructive to compare this expression with that for a *single* cavity of length $L = cNT$:

$$x(L = cNT) = x_1 e^{i\lambda_1 NT} = \frac{1}{D}\left[a_0 + C_x x_0 + C_y y_0\right] e^{i\lambda_1 NT}. \tag{19}$$

We see that in either case the growth rate is the same, and is proportional to the number of cavities. The difference is quantitative, and lies in the numerical pre-factors:

$$\frac{a_1^N}{a(L = cNT)} = \left(\frac{C_x + i\lambda_1 C_y}{D}\right)^{N-1}. \tag{20}$$

The factor $\left(C_x + i\lambda_1 C_y\right)/D$ is typically of order unity, and for reasonable values of N (~5), there is only around an order of magnitude decrease in the amplitude of the final radiation field.

Multiple bunches. Next consider a second bunch passing through the FEL. As it enters the first cavity it has the same bunching as did the first bunch (typically none, unless a prebuncher is used), so that the initial conditions are $x_{in} = x_0$ and $y_{in} = y_0$. However, the initial radiation field is *not* a_0. In its passage through the first cavity the first bunch left behind radiation of amplitude a_1^1 given by Eq. (16). This radiation bounces off two walls before being seen by the second bunch (assuming the spacing between bunches is equal to twice the length of the cavity). Modelling the

loss at each wall by a reflection coefficient R, the initial value of the radiation field seen by the second bunch entering the first cavity is $a_{in} = R^2 a_1^1$.

One can now use Eq. (12) to calculate the quantities x_2^1, y_2^1 and a_2^1 for the second bunch at the end of the first cavity. At the entrance to the second cavity, the initial values of the bunching are those at the end of the first cavity $\left(x_2^1 \text{ and } y_2^1\right)$ while the initial value of the radiation is determined by that left behind in the cavity by the previous bunch $\left(R^2 a_1^2\right)$. Proceeding thus we can write down, with some effort, a general expression for the M^{th} bunch at the end of the N^{th} cavity:

$$x_M^N = \frac{\left(R^2\right)^{M-1}\left(\lambda_1^2\right)^{M-1}}{D^{M+N-2}} \cdot \frac{N(N+1)\ldots(N+M-2)}{(M-1)!}\left(C_x + i\lambda_1 C_y\right)^{N-1} \times \\ \times x_1(a_0, x_0, y_0) e^{i\lambda_1 (M+N-1)T}, \tag{21}$$

with $y_M^N = i\lambda_1 x_M^N$ and $a_M^N = \lambda_1^2 x_M^N$.

Again, to compare with the expression for the M^{th} bunch at the end of a *single* cavity of length $L = c(NT)$,

$$x_M(L = cNT) = \frac{\left(R^2\right)^{M-1}\left(\lambda_1^2\right)^{M-1}}{D^{M-1}} \cdot x_1(a_0, x_0, y_0) e^{i\lambda_1 MNT}. \tag{22}$$

We notice a big difference between the growth-rates in the two cases. For a single-cavity FEL the growth rate goes as the product of M and N, whereas for the multi-cavity it goes much slower—only as their sum. However, Eq. (21) tells us that in the MC/FEL there is still exponential growth. Though this growth may be slower than in the single-cavity case, we have derived the advantage of getting around the problem of gain degradation due to slippage effects. Further, since these effects are not included in Eq. (22) for the single-cavity FEL, the comparative performances of multi- and single-cavity FELs would be more equitable than Eqs. (21) and (22) suggest.

Because of the slower growth-rate, a MC/FEL would require operation with a greater number of bunches than would a single-cavity FEL. However, because the cavity length is now

smaller, the bunches can be more closely spaced. The total pulse width would therefore be the same ($\propto MN$), but not, of course, the average current (or charge) in a pulse.

The above analysis, in the exponential regime, is simple and revealing, and indeed provided the original motivation for the concept of a MC/FEL. However we found, in multi-particle simulations, that for practical parameters this regime seldom persists for periods long enough that a comparison may be made between theory and simulation. Usually, the system starts out in the lethargy regime, where all three eigen-functions contribute, and very quickly reaches the non-linear regime. In the next sub-section, therefore, we look at the lethargy regime.

C. Lethargy Regime

We now turn our analysis to the lethargy regime, in which all three eigen-values contribute comparably, and the approximation leading to Eq. (12) can no longer be made. We therefore go back to the general solutions, Eq. (10). Here we expand the exponentials in those equations and, arguing that the growth is slow, keep terms only up to the cubic (the usual approximation). Further, we assume that the detuning is small, so that the terms proportional to δ and ρ in Eq. (7) can be neglected. Then the eigenvalues are just those derived in standard treatments (e.g. Colson [4]),

$$\lambda_1 = -i\omega\frac{i+\sqrt{3}}{2} \tag{23a}$$

$$\lambda_2 = -i\omega\frac{i-\sqrt{3}}{2} \tag{23b}$$

$$\lambda_3 = -\omega\,, \tag{23c}$$

where

$$\omega = \left(\frac{j}{2}\right)^{1/3}\frac{c}{2\omega_0 L}, \tag{24a}$$

and j is the dimensionless current density given by [4]:

$$j = \frac{\left(4L^2\omega_0 e\kappa\right)^2 n_0}{\gamma_0^3 mc^4}. \tag{24b}$$

Using the explicit forms of the eigenvalues, and using the initial conditions $x = x_{in}$, $y = y_{in}$ and $a = a_{in}$ at $\tau = 0$, the solutions in this regime, within the framework of the approximations made above, can be written as

$$x = x_{in}\left[1 + \frac{i}{6}\omega^3\tau^3\right] + y_{in}\tau - \frac{a_{in}}{2}\tau^2 \tag{25a}$$

$$y = x_{in}\left[\frac{i}{2}\omega^3\tau^2\right] + y_{in}\left[1 + \frac{i}{6}\omega^3\tau^3\right] - a_{in}\tau \tag{25b}$$

$$a = -x_{in}\left[i\omega^3\tau\right] - y_{in}\left[\frac{i}{2}\omega^3\tau^2\right] + a_{in}\left[1 + \frac{i}{6}\omega^3\tau^3\right]. \tag{25c}$$

We could now proceed as we did in the previous section, considering first a single bunch through N cavities and then M bunches. Unfortunately, the analysis is now much more complicated, and it turns out not to be possible to write down a general expression for N cavities and M bunches. To simplify matters and to facilitate comparison with simulation, we consider the case when there is no pre-bunching, i.e. $x_0 = y_0 = 0$. Then, proceeding as in the previous sub-section, and in the same notation, the value of the radiation for the M^{th} bunch at the end of the N^{th} cavity can be written as

$$a_M^N = \left(R^2\right)^{M-1} a_0\left[1 + i\omega^3 T^3\left(MN - 2(M-1)\right)\right]. \tag{26}$$

Here we have retained only the lower-order terms in an expansion in $\omega^3 T^3$, and consequently these expressions are only valid for small M and N ($\lesssim 10$). Eq. (26) can be rewritten in terms of the power ($P = a^* a$):

$$P_M^N = P_0\left(R^2\right)^{2M-2}\left[1 + \left(MN - 2(M-1)\right)^2\omega^6 T^6\right], \tag{27}$$

where P_0 is the initial input power into the first cavity.

Since, in any practical realization of the MC/FEL, a large number of bunches will be needed to achieve saturation, we now consider the opposite limit, i.e. when M and N are very large. From this macroscopic point of view, within a single cavity, during a single pass, the power level can be taken to be approximately constant. Similarly, the bunching within a particular cavity is negligible compared to the cumulative effect of bunching over many cavities. Consequently, one can identify two distinct time-scales of importance in the problem. One, say z, measures distance along the MC/FEL and is proportional to N, the number of cavities. The other, say t, measures time from pass to pass and is proportional to M, the number of bunches. Further, since the bunching changes only down the MC/FEL and starts afresh for each new bunch, its direct dependence is only on z. Similarly, since the radiation within a particular cavity does not couple to that within another cavity (except via the electron beam), its direct dependence is only on t.

With these considerations in mind Eq. (25) can be replaced, in the continuous limit, by partial differential equations that give the variation of x and y as a function of z and of a as a function of t:

$$\frac{\partial x}{\partial z} = y(t,z) \tag{28a}$$

$$\frac{\partial y}{\partial z} = -a(z,t) \tag{28b}$$

$$\frac{\partial a}{\partial t} = -i\omega^3 x(t,z), \tag{28c}$$

where we have kept only the lowest-order terms in $\omega^3 T^3$. Solving these equations in the asymptotic limit and extracting only the leading order term, one finds that $a(z,t) \sim \exp\left[\alpha z^{2/3} t^{1/3}\right]$, where α is some undetermined constant. Interpreting z as N and t as M, one can write for the power P,

$$P \sim \exp\left[2\alpha N^{2/3} M^{1/3}\right]. \tag{29}$$

Eqs. (27) and (29) give predictions for the dependence of the power level upon M and N in two different limits. We now turn to multi-particle simulations to test these predictions in the lethargy regime, and to explore the behavior of the system in the nonlinear regime.

4. Numerical Simulations

In this section, we numerically study the performance of three MC/FELs. The full nonlinear equations of motion given in Eq. (1) are used in the simulations. Parameters for the three MC/FEL examples are listed in Table 1. In all these cases, the reflection coefficient R is taken to be equal to 0.98. However, the reflection coefficient for the right-hand wall of the output (i.e., final) cavity is taken to be equal to 0.95 to allow for outcoupling of radiation.

Before proceeding further, we first verify the theoretical prediction given in Eq. (27). A comparison of the theory with numerical simulation is given in Fig. 2. We see that the power output predicted by theory agrees well with that found in simulations. The agreement is good even when there is a net loss of power due to reflections (see Fig. 2b). However, the agreement starts getting worse as we go to larger values of M and N. Next, we check the prediction given in Eq. (29). Since Eq. (29) is an asymptotic formula and we have only a few cavities, we are not able to check the dependence on cavity number N. However, we have verified the dependence on M for a fixed N. With these comparisons, we have enough confidence in the validity of the MC/FEL concept to embark on a detailed numerical study.

First, we obtain the power output from a single optical cavity with the wiggler length given in Table 1. In contrast to conventional FEL oscillators, the length of the optical cavity is equal to the wiggler length in our case. Next, we study a MC/FEL whose total length is equal to the length of the single cavity considered above. The length of individual optical cavities in the MC/FEL is taken to be slightly smaller than the slippage length. All other parameters remain the same. The first (N-1) cavities are used to bunch the electrons. Output power is extracted from the final (N^{th}) cavity.

In the final two rows of Table 1, we compare the output power obtained in a single long cavity with that obtained in the corresponding MC/FEL. In all three examples studied, we see that the power output in the final cavity of the MC/FEL is larger than the power output in a single long cavity. A more detailed comparison of the power evolution in the two cases is given in Figs. 3 and 4. Only the second example (λ_s = 100 μm) is considered. Figure 3 shows the evolution of power as a function of electron bunch number in the single cavity case. Figures 4a, 4b and 4c show the corresponding evolution in cavities 1, 4 and 7, respectively, for the MC/FEL. As noted earlier, power output in the final cavity of the MC/FEL (see Fig. 4c) is higher than the corresponding power output in a single long cavity (see Fig. 3). We observe that the MC/FEL works despite losing power in the first cavity (see Fig. 4a). This is because the first cavity manages to bunch the electrons slightly even though it is losing power. Figures 5a and 5b show the evolution of the bunching factor $\left|\left\langle e^{i\theta}\right\rangle\right|$ in a MC/FEL. As expected, the bunching factor is seen to increase both as a function of cavity number and bunch number.

In Section 3 we have provided formulae for the power achieved in two different approximations: Eq. (27) in the limit of small ($\lesssim 10$) M, N, and Eq. (29) in the limit of very large M, N. The actual saturated power obtained in the numerical simulations can also be estimated. Assuming that the incoming electron beam sees a static potential "bucket" at saturation, and assuming that the maximum energy lost by an electron is equal to the bucket height, one can show [5] that the extraction efficiency (for a single electron) is given by $\eta = \frac{1}{2N_w}$, where N_w is the number of wiggler periods. Then, if the power in the electron beam is P_{beam}, the saturated power level is given by,

$$P_{sat} = \frac{1}{2N_w} P_{beam} . \qquad (30)$$

It is important to note here that N_w is the number of wiggler periods *within the last cavity*, and not of the MC/FEL as a whole.

Applying this formula to the three numerical examples considered in this section, we find the estimated saturation levels to be 3, 12 and 6 MW, respectively, as compared to the actual saturation levels of 3.5, 8 and 4 MW, respectively. The estimates are thus quite good.

5. Conclusions

There are a number of conclusions to be drawn from this work:

First, that the concept (see Fig. 1) of a Multi-Cavity Free-Electron Laser (MC/FEL) is a valid concept, i.e., that a MC/FEL can be expected to work.

Second, that a MC/FEL will overcome the slippage between radiation and particle beam so that it can produce radiation pulses as brief as electron pulses (even when slippage would suggest that the radiation pulse is longer than the particle pulse).

The third conclusion is that the peak power produced in a MC/FEL can be even higher than in a single cavity FEL, because the saturation condition implies that power increases as the optical cavity is reduced in length. In practice one should design an FEL so that the optical cavity is made as short as possible, while still having a net gain per pass, so as to produce the maximum peak power.

Further work of a theoretical nature, which remains yet to be done, is to study the concept in 2D, including diffraction phenomena, proper study of optical mode structure and reflectivity, etc. (We don't expect the principle of the MC/FEL to be modified, but the "real numbers" will surely be different.)

Finally, then, it seems likely that MC/FELs will provide an interesting new capabilty of FELs. First, however, some experimental study of the concept is called upon.

References

1. J. Masud, et al Phys. Rev. Lettr. **58**, 763 (1987).
2. N. A. Vinokurov, "The Optical Klystron Theory and Experiment", dissertation of The Institute of Nuclear Physics, Novosibirsk (1986).
3. R. Bonifacio, C. Pellegrini, and L. Narducci, Optical Comm. **50**, 373 (1984).

4. W.B. Colson, in Laser Handbook, vol. 6, edited by W.B. Colson, C. Pellegrini and A. Renieri, (North-Holland, Amsterdam, 1990) p. 115.

5. N.M. Kroll, P.L. Morton and M.N. Rosenbluth, IEEE J. Quantum. Electron., **QE-17**, 1436 (1981).

Table 1.
Three examples of Multi-Cavity Free-Electron Lasers

Parameters	First Example	Second Example	Third Example
$\lambda(\mu m)$	10	100	1000
τ_{pulse} (ps)	1	2	10
λ_w (cm)	1.0	2.0	2.5
a_w	1.0	1.0	1.0
Wiggler length (m)	1.5	0.7	0.3
Cavity length (cm)	25	10	5
N	6	7	6
r_{beam} (mm)	1.0	1.0	1.0
I_{peak} (A)	5	10	5
γ	27.4	12.2	4.3
Slippage length (cm)	30	12	7.5
ρ	$3x10^{-3}$	$1x10^{-2}$	$3x10^{-2}$
P_{beam} (MW)	140	124	22
P_{out} (MW)	3.5	8.0	4.0
P_{out} (MW) (for single cavity)	1.2	2.6	1.2

Figure Captions

Figure 1: Conceptual layout of a multi-cavity FEL.

Figure 2: Normalized power output (P_{out}/P_{in}) as a function of bunch number in the second cavity of a multi-cavity FEL. The parameters used are those given for the second example in Table 1. Results from the theory (Eq. 27) and numerical simulation are compared. Figures 2a and 2b differ in the value of reflection coefficient (R) used for the cavity walls. Figure 2a is for $R = 1.0$ and Figure 2b is for $R = 0.98$.

Figure 3: Power output as a function of bunch number for a single optical cavity whose length is equal to the total wiggler length of the corresponding multi-cavity FEL. All other parameters used are those given for the second example in Table 1.

Figure 4: Power output in a multi-cavity FEL. The parameters used are those given for the second example in Table 1. Figures 4a, 4b and 4c show the power output as a function of bunch number in the first, fourth and seventh cavity, respectively.

Figure 5: Evolution of the bunching factor $\left|\left\langle e^{i\theta}\right\rangle\right|$ in a multi-cavity FEL. The parameters used are those given for the second example in Table 1. Figure 5a shows the bunching factor at the end of the last cavity as a function of bunch number. Figure 5b shows the bunching factor for the last bunch as a function of cavity number.

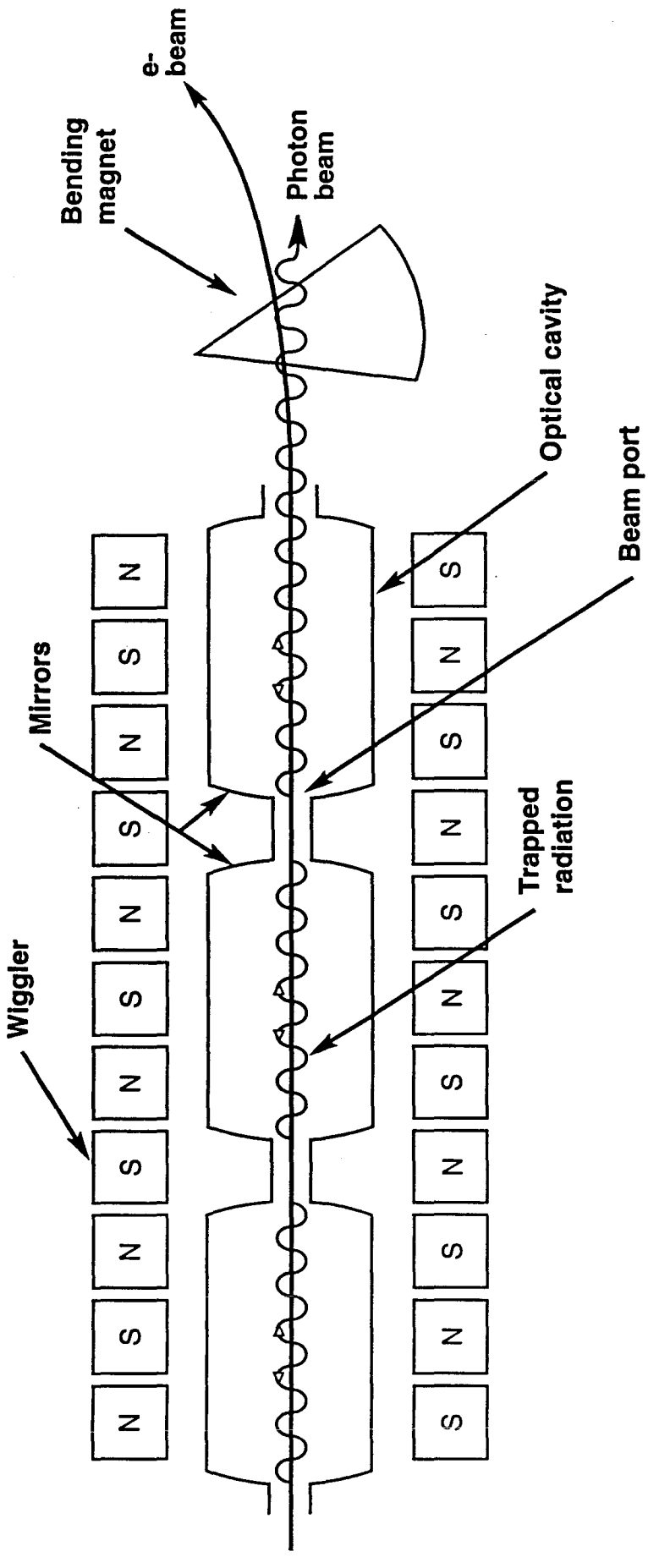
e-
beam
Bending
magnet
Photon
beam
Optical cavity
Beam port
Mirrors
Trapped
radiation
Wiggler
N
S
N
S
N
S
N
S
N
S
S
N
S
N
S
N
S
N
S
N

Fig. 1

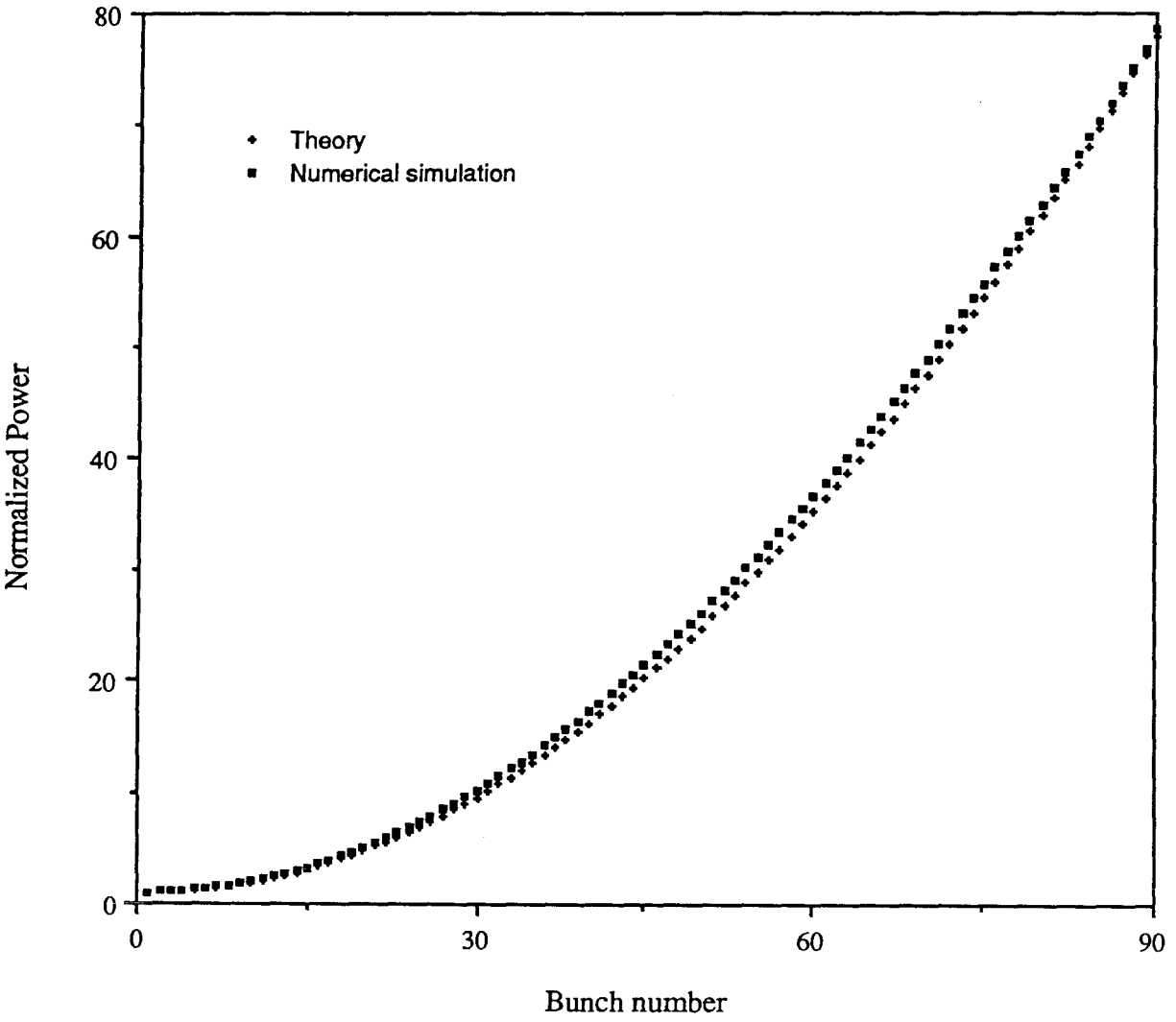
80
60
40
20
0
Normalized Power
Theory
Numerical simulation
0
30
60
90
Bunch number

Fig. 2a

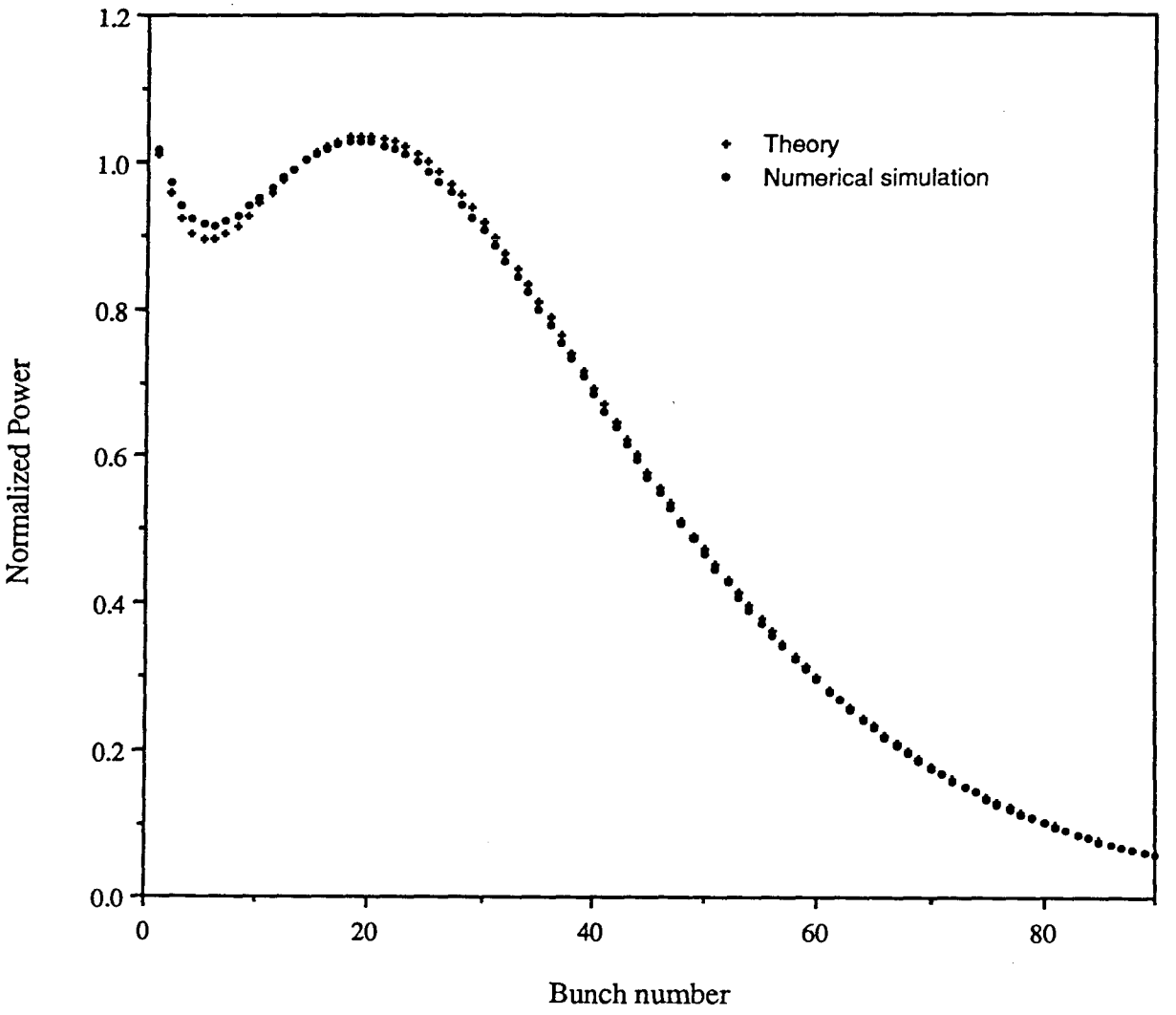
1.2
1.0
0.8
0.6
0.4
0.2
0.0
Normalized Power
0
20
40
60
80
Bunch number
Theory
Numerical simulation

Fig. 2b

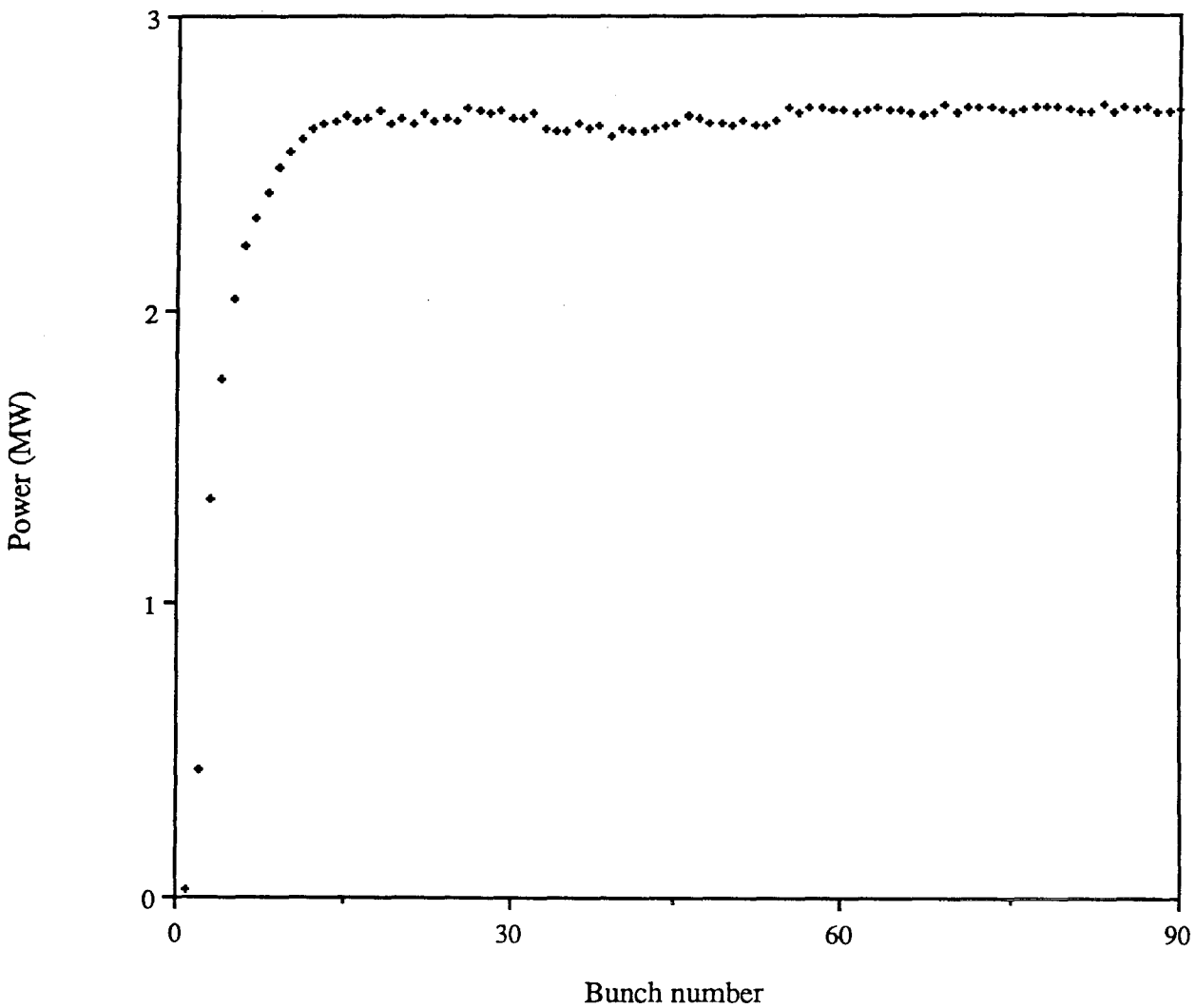

Fig. 3

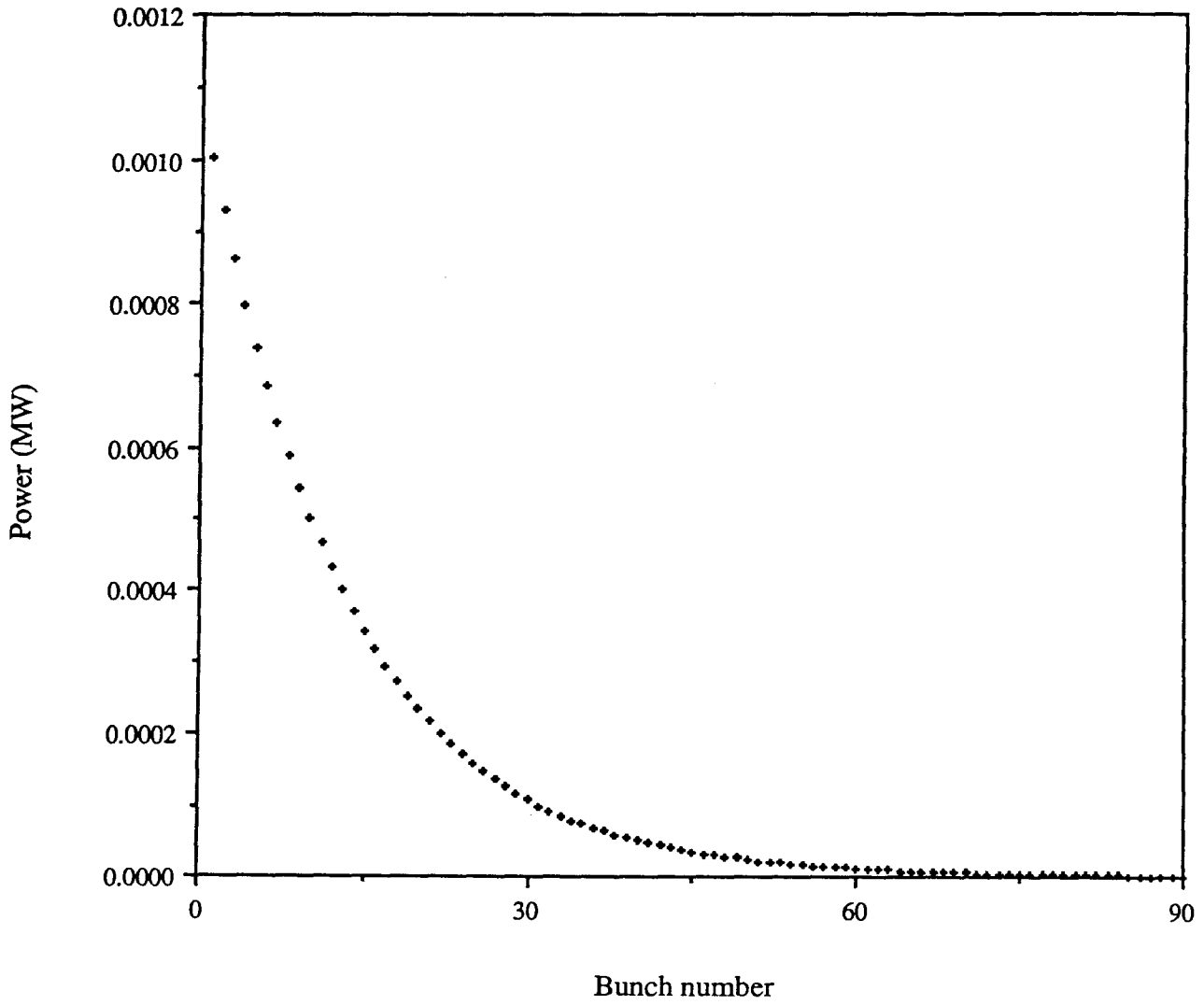
0.0012
0.0010
0.0008
0.0006
0.0004
0.0002
0.0000
Power (MW)
0
30
60
90
Bunch number

Fig. 4a

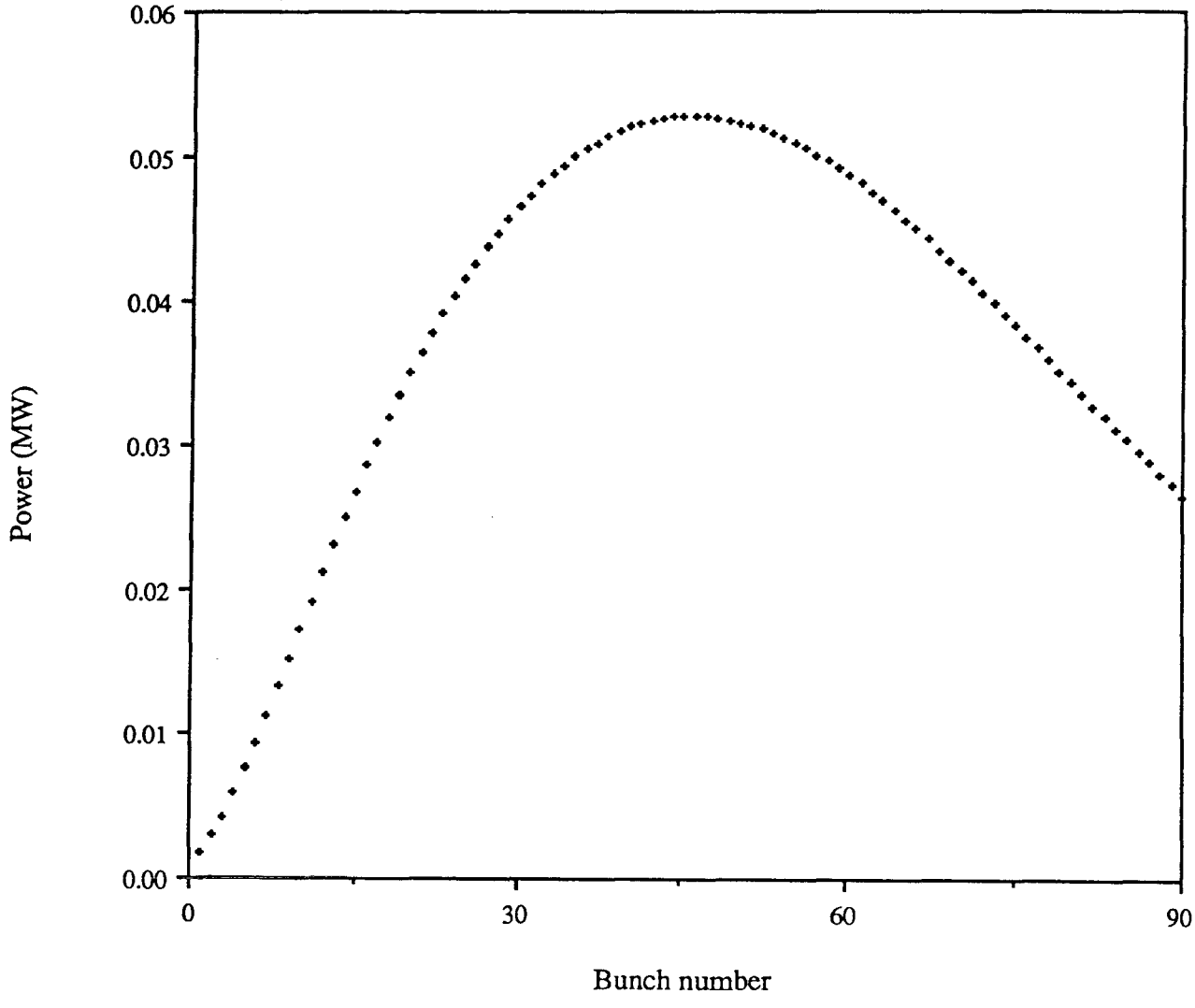

Fig. 4b

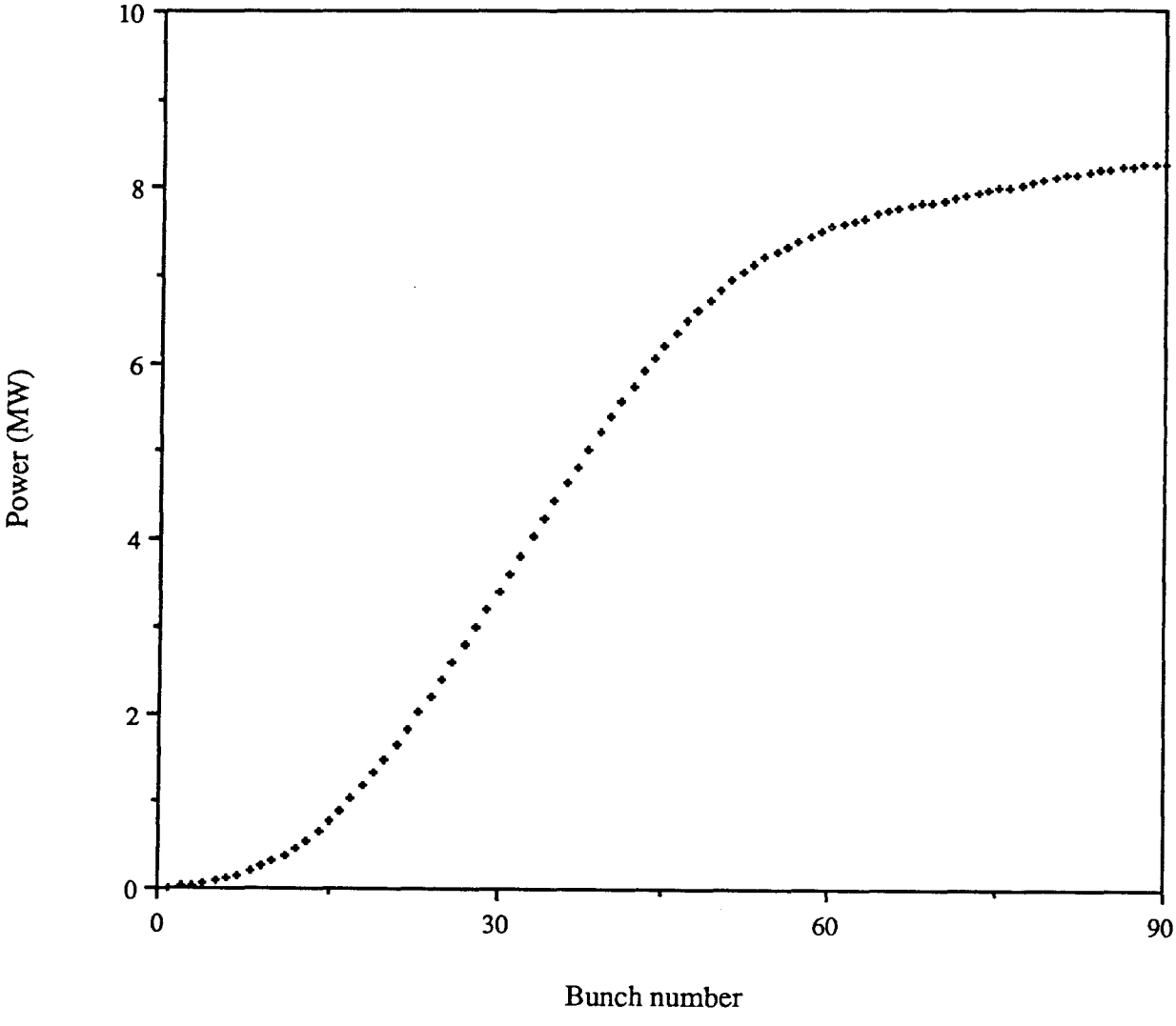

Fig. 4c

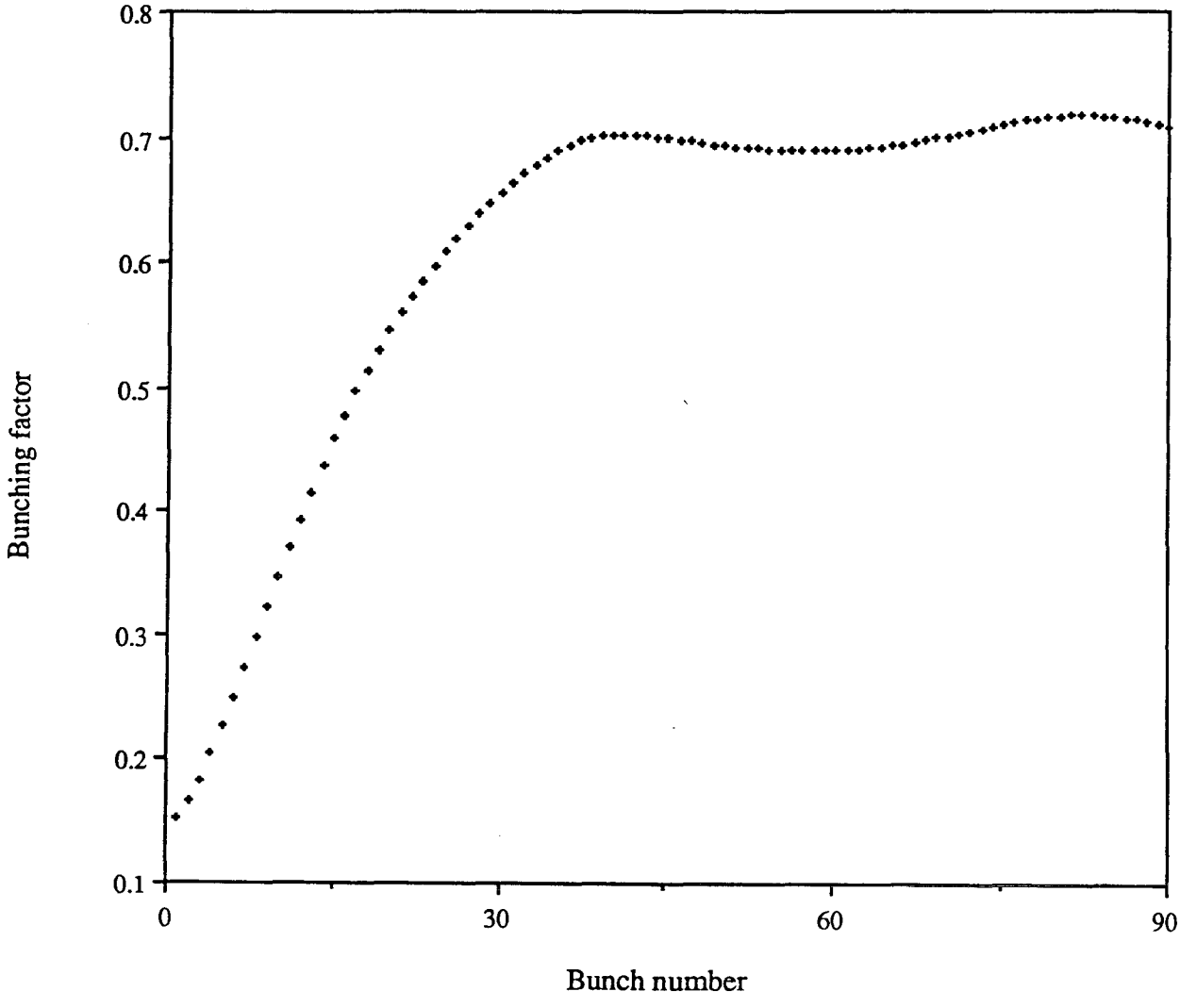

Fig. 5a

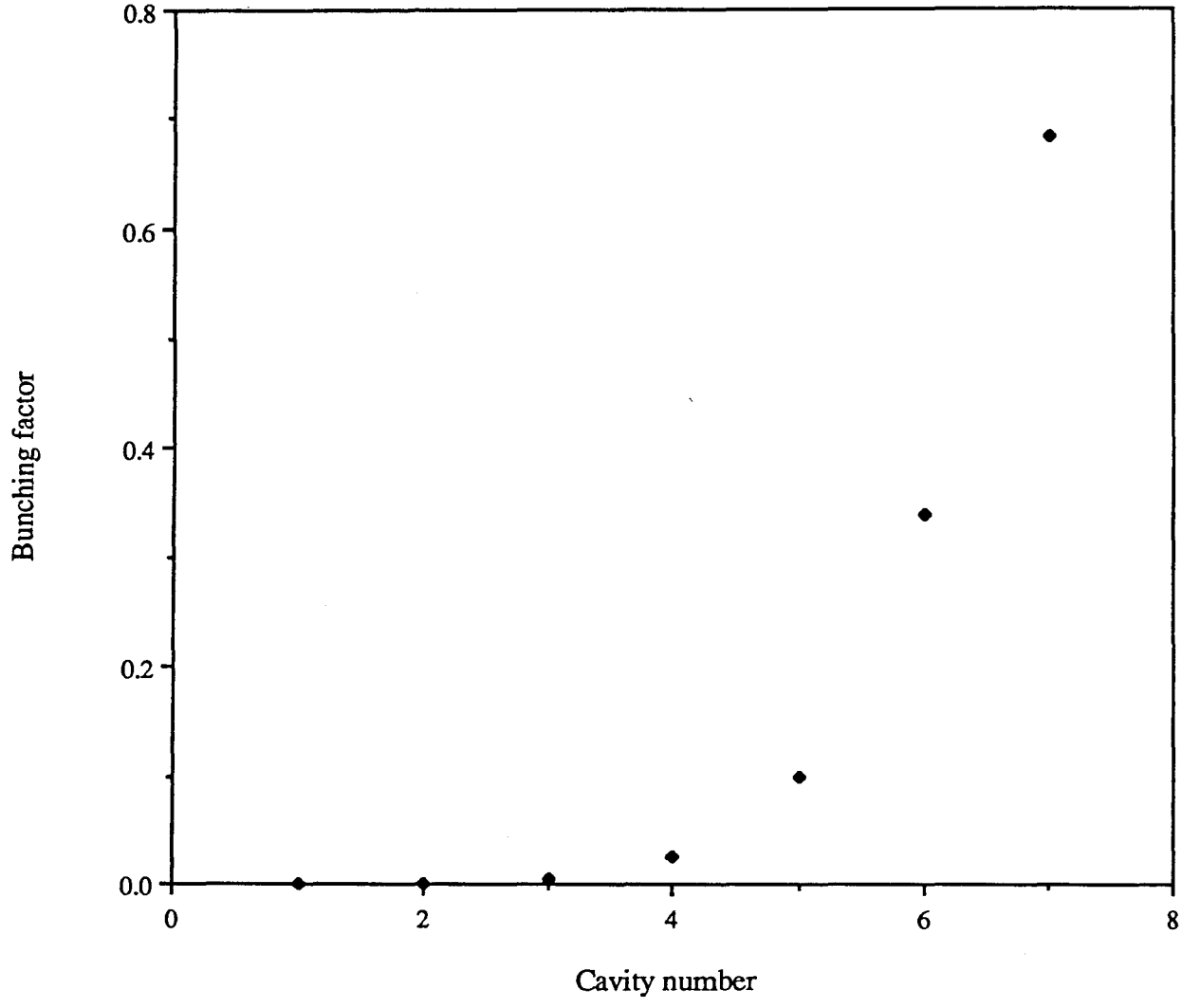

Fig. 5b